Theor Chem Acc (2011) 130:27–36
DOI 10.1007/s00214-011-0955-3

REGULAR ARTICLE

Measuring electron sharing between atoms in first-principle simulations

Giovanni La Penna · Sara Furlan · Miquel Solà

Received: 29 December 2010 / Accepted: 30 April 2011 / Published online: 19 May 2011

Abstract Calculations of large scale electronic structure within periodic boundary conditions, mostly based on solid state physics, allow the modeling of atomic forces and molecular dynamics for atomic assemblies of 100–1000 atoms, thus providing complementary information in material and macromolecular sciences. Nevertheless, these methods lack connections with the chemistry of simple molecules as isolated entities. In order to contribute to establish a conceptual connection between solid state physics and chemistry, the calculation of the extent of electron sharing between atoms, also known as delocalization index, is performed on simple molecules and on complexes with transition metal atoms, using density functional calculations where the Kohn–Sham molecular orbitals are represented in terms of plane waves and in periodic boundary conditions. These applications show that the useful measure of electron sharing between atomic pairs can be recovered from density functional calculations using the same set-up applied to large atomic assemblies in condensed phases, with no projections of molecular orbitals onto atomic orbitals.

Keywords Density-functional theory · Delocalization index · Computer simulations

G. La Penna
National Research Council of Italy, Institute for Chemistry of Organo-Metallic Compounds, via Madonna del Piano 10, 50019 Sesto Fiorentino, Firenze, Italy
e-mail: glapenna@iccom.cnr.it

S. Furlan
National Center for Scientific Research, Laboratory of Coordination Chemistry, 205 route de Narbonne, 31077 Toulouse, France
e-mail: sara.furlan@gmail.com

M. Solà (✉)
Institute of Computational Chemistry and Department of Chemistry, University of Girona, Campus Montilivi, 17071 Catalonia, Girona, Spain
e-mail: miquel.sola@udg.edu

1 Introduction

The investigation of the electronic ground state structure of large atomic assemblies, both as isolated molecules, clusters and condensed phases, is becoming a routine application because of the many improvements in density functional theory (DFT) [1–3]. To cope with the size of assemblies, like surfaces or nanotubes, and with solvents in the liquid state, and to minimize the effects of the finite size of modeled samples, periodic boundary conditions (PBC) are adopted. Therefore, most of the modern tools for such investigations come from solid state physics. The Kohn–Sham (KS) molecular orbitals (MOs) used in DFT as tools for representing the electron density [4, 5] are represented as Fourier series: the KS MOs are expanded in a large number of plane waves (PW) with space periodicity associated to the cell used in the calculation as the sample. In this basis-set, the evaluation of integrals is relatively easy and the transformation from reciprocal (PW) space into real 3-d space of quantities (first of all the electron density) is efficient because of the implementation of fast Fourier transform (FFT) numerical techniques on parallel computers.

The interactions between valence electrons represented with such diffuse functions with the atomic cores are, in most of the cases, introduced via pseudopotentials. The advent of the ultrasoft pseudopotential (US-PP) [6] together with algorithms for efficient implementations of them

(like double grids) [7], allow the use of a relatively small number of PW functions in the construction of the basis-set and in most of the intensive calculations. As a result, the size of the finite element representing the electron density in the real space can be as small as 10 pm for systems of hundreds or thousands of atoms in cells with a side of 10 nm.

This theoretical description of electron density allows a high numerical efficiency and, as a consequence, the possibility of using the same description for interatomic forces and for first-principle molecular dynamics [8], thus opening the possibility of collecting wide statistics for atomic configurations and of exploiting the dynamics of extended systems.

The disadvantage of the PW description is in the difficulty of understanding the results of calculations (electron density, frontier molecular orbitals, collective properties) in terms of atomic contributions, chemical bonds, and their perturbations [9]. The chemical nature of the elementary components of the sample is lost when a diffuse representation for the electron density is adopted and most of the information about atoms is encoded in the ultrasoft pseudopotential.

In recent years, many theoretical descriptions of electronic structure were developed aiming at measuring the extent of electron sharing between two or more atoms in complicated molecules. These efforts are particularly necessary when several transition metal atoms are involved [10]. Most of the available tools for describing via atomic contributions the electronic structure, reside on basis-sets where atomic functions are mixed with diffuse contributions (like in the linearized augmented PW basis-set implemented in the Wien2k package [11]). In this case, the topological analysis of electronic structure can be performed [12] similarly to the calculations based on localized atomic basis-sets used for isolated molecules. On the other hand, in those cases where the basis-set does not include atomic orbitals explicitly, suitable projections of PW representations of KS MOs must be performed [13].

In this work, we aim at applying direct measures of electron localization and delocalization, a concept first introduced in Refs. [14–16] and then developed to represent the chemical bonding in aromatic systems, complex molecules, and in condensed phases (see Refs. [17–19] and references therein). The work we report here, is a further step toward the goal of providing a parameter measuring electron delocalization independently from the basis-set adopted for the calculation of the wave function. More recently, the variance–covariance analysis of total electron density ends up with the same set of simple parameters, that allow to measure the amount of shared electrons between any pair of atoms in a system described by a set of occupied molecular spin orbitals, both at Hartree–Fock, DFT, and correlated levels [19–21]. These parameters were called localization and delocalization indices (DIs), and are calculated in terms of molecular (or natural) orbitals as:

$$\lambda(A) = \sum_{i,j} [n_{i,\alpha} n_{j,\alpha} + n_{i,\beta} n_{j,\beta}] S_{i,j}(A)^2, \tag{1}$$

$$\delta(A,B) = 2 \sum_{i,j} [n_{i,\alpha} n_{j,\alpha} + n_{i,\beta} n_{j,\beta}] S_{i,j}(A) S_{i,j}(B), \tag{2}$$

where i and j run over all the occupied molecular spin orbitals, $S_{i,j}(A)$ are overlap integrals of the ith and jth spin orbitals, integrated within the region of space identified as the basin of atom A, and $n_{i,\alpha}$ are the occupations of each spin orbital. In our work, the orbital occupations, $n_{i,\alpha}$ and $n_{i,\beta}$, are equal to one or zero depending on whether the molecular spin orbital is occupied or not. Delocalization index is the bond order defined in Eq. (9) of Ref. [16], while localization index is a shifted version of the atomic valence index in Eq. (10) of [16]. Localization and delocalization indices are dimensionless, being expressed in terms of number of electrons.

Delocalization indices are not a measure of the strength of the bond between the pair of atoms involved. This latter measure is given by the force constant, accurately derived from the second derivatives of the energy with respect to atomic displacements. DIs provide a complementary information, being these latter a measure of the covalent character of the interaction between the given pair of atoms [22–24], also readable as the number of "Lewis-type" electron pairs involved in the interaction. The combination of the information of force constants and DIs allows to classify the interaction as covalent (DI $>$ 0) or electrostatic and/or dispersive (DI $\sim$ 0).

The measure of localization and delocalization, λ and δ, respectively, resides on the identification of atomic basins. This partition of space can be performed by several different methods [25]. The one we adopted in this work is the topological partitioning based on the quantum theory of atoms in molecules (QTAIM), initially proposed by Bader [26]. Other methods can be alternatively used [27, 28]. The first comparison between topological and Hilbert space partitioning [16] showed that with the former partitioning the dependence of results from the basis-set is dramatically reduced.

Despite other tools for analyzing electron density can be applied to PW-based DFT calculations (like the TOPOND program [29] based on the crystal package [30]), these tools do not allow the direct calculation of the delocalization index so far. The typical analysis of bonds performed by QTAIM [10, 26], relies on the identification of bond critical points and bond paths, but this analysis requires a higher spatial resolution compared to the direct evaluation of delocalization index, as it is reported in this work.

The detailed balance of electron sharing between atoms is guaranteed by the relationship:

$$N(A) = \lambda(A) + 1/2 \sum_{A \neq B} \delta(A, B), \quad (3)$$

where $N(A)$ is the integral of electron density within the basin A, i.e., the sum of the core charge and of the valence electron density on atom A, as it is identified, in this case, by the QTAIM analysis.

In this work, we apply the equation for the delocalization index to DFT calculations where the Kohn–Sham molecular orbitals are represented in terms of plane waves, as this is the usual set-up for large scale electronic structure calculations and first-principle molecular dynamics simulations. The applications range from simple molecules to molecules where the nature of bonds, especially when transition metal atoms are involved, is less well defined. The aim of this work is to measure the number of electrons shared between atoms adopting, for the different systems, the same conceptual and computational framework of solid state physics used to evaluate atomic forces. The result is that the DIs are only slightly dependent of the basis-set adopted for DFT calculations. No projections of valence molecular orbitals onto atomic orbitals is performed at any step of the calculation.

2 Methods

Most of the DFT calculations presented here were performed with the Quantum–Espresso package [31]. The DFT PW calculations were performed with $K = 0$ (the so-called Γ-point), i.e., no effects of the periodicity over length-scales larger than the super-cell dimensions were included. With the exception of the ionic lattices of NaCl, LiF and NaCN, the initial configurations of each molecule were placed in a cell with a size leaving a minimal distance of 0.5 (for neutral cells) and 0.8 (for charged cells) nm between the atoms in neighboring cells. These distances were found sufficient for mimicking isolated conditions [7] when Ewald techniques are used for treating electrostatics [32, 33]. The NaCl and LiF configurations were built in the *fcc* lattice and up to eight unitary cells arranged in the $2 \times 2 \times 2$ 3-d lattice were used in the calculation. The minimal distance between ions was 2.842 and 2.027 Å for NaCl and LiF, respectively. The $Pt_3(CO)_6^{2-}$ isolated anion was built according to the D_{3h} symmetry group and with distances and angles derived from the crystal structures (see Ref. [34] and references therein).

The geometry of each molecule was optimized by minimizing the energy of the system. Except for the convergence tests, the energy cut-off for the PW basis-set was 25 Ry, while the energy cut-off for the finer grid (mostly used in calculations involving valence-core interactions) was 250 Ry. The Perdew–Burke–Ernzerhof (PBE) exchange–correlation functional was used in all the DFT calculations [35], with US-PP developed accordingly.

Since a standard Ewald sum technique is used in the calculation of interatomic forces, a neutralizing uniform background charge is added to the system [32, 33, 36]. Therefore, super-cells with a net charge (like cyanide and the $[Pt_3(CO)_6]^{2-}$ anion) and with periodic images farther than 0.8 nm, are minimally affected by spurious Coulomb repulsion within periodic images. The energy of charged systems is computed by using suitable corrections when PW basis-set is used [32, 33, 37]. In some of these corrections, the electron density and atomic forces are also corrected [32, 33], thus affecting geometry optimization results. In the spin-polarized cases ($S_z > 0$), the DFT calculations are performed within the local spin density approximation.

Approximated all-electron densities were analyzed with the QTAIM approach for identifying the set of points in space confined within the surfaces of zero flux of the electron density gradient. This analysis was performed with the algorithm initially proposed by Sanville et al. [38, 39]. The version 0.29a of the code was used in this work. Once the atomic basins were identified, the integrals in Eq. (2) for DIs were computed simply by summing over the set of elementary cubic volumes identified by each of the atomic basins. Therefore, the implementation of Eq. (2) requires the simple collection of 3-d grids of the valence electron density and of the set of KS molecular orbitals representing it. In this work, the 3-d grids are represented as Gaussian cube-files.

In most cases, the valence electron density was collected in real space on the finer 3-d grid (i.e., with a finite element side of about 10 pm, corresponding to the larger PW energy cut-off of 250 Ry). By increasing the latter energy cut-off, a finer grid for representing valence electron is achieved, therefore assessing the convergence of Eq. (2) by increasing the resolution of electron density and KS molecular orbitals. In all cases, the valence electron density was completed with the core electron density. The angular-averaged approximated radial part of groups of core states [40–42] was sampled with a finer grid (from 4 to 16 cubes within each of the cubes used in the finer valence density grid) and within a 3 bohr core-radius away from each nucleus. The average density obtained with this sampling within each valence density cube was added to the corresponding valence cube. This procedure is a smoothing of the core electron density within each valence electron density cube containing at least one point within 3 bohr from each nucleus. The correctness of integrals of the all-electron density in all cases was checked to be within 1%.

Some of the results for simple molecules reported here for comparisons, were obtained with ADF [43] codes. In the ADF case, the PBE exchange–correlation functional [35] was used together with a triple-ζ Slater-type orbitals (STO) basis-set with two sets of polarization functions (the so-called TZ2P basis-set in ADF). For comparisons between all-electron results and approximated treatments of core-valence interactions, the core electrons of atoms were, in some cases, treated as frozen cores. A similar ADF set-up was used for calculating bond multiplicities, recently implemented in ADF [44].

3 Results

3.1 Convergence analysis

The low resolution of electron density and of KS MOs obtained in PW representations deserves a convergence assessment of Eq. (2) and of the QTAIM partitioning of space, by using simple molecules. In the following, we report results for CO and for the cyanide anion.

Results obtained for δ(C,O) with different localized basis-sets and 3-d grid resolutions are reported in Table 1. The identity of DIs when core states are included or not in Eq. (2) (AS and VS, respectively), indicates that core states do not contribute to electron sharing, like expected, being the core states highly localized on their respective atom. Different localized basis-sets used within the ADF code shows that the effect of the used real-space resolution in space partitioning and in the integrals of Eq. (2) is more significant than a change in basis-set or in atomic core approximation. The difference between these data and those reported in Refs. [16] and [20], these latter in the range 1.51–1.57, can be attributed to the HF level of theory, as already discussed in the literature [20]. However, the differences within this set of data is smaller than that provided by a different partitioning (see Table 1 in Ref. [16]). The Hilbert space partitioning provided, with the same basis-sets and geometry, values in the range 2.31–2.32. The agreement between the delocalization index calculated with 3-d grids and those reported in the literature [20, 45], these latter evaluated with accurate methods and basis-sets, shows that for a grid size of about 5 pm the accuracy on DI is within 0.1 units. Despite the effect of the frozen core is negligible, it must be remarked that the electron density is, in all the cases reported in Table 1, described by all the electrons. The QTAIM analysis of valence electron density is not rigorous and provides significantly different results compared to that of the all-electron density. Errors in the definition of the zero-flux surface for electron density when atomic cores are neglected are mainly due to the inaccuracy of density gradient when empty regions (atomic cores) are sampled. These numerical instabilities are removed introducing even coarse-grained representations of atomic cores (see Sect. 2).

Once a satisfactory level of accuracy was found for the 3-d grid approximation of integrals using localized basis-sets, a convergence analysis was performed on δ(C–O)

Table 1 Delocalization index, δ in Eq. (2), for CO from calculations using atom-centered basis-sets, with different DFT set-up and with different 3-d grid resolution of charge density and KS molecular orbitals

Basis-set	C–O distance (Å)	ΔE (kJ/mol)	Side of elementary volume (bohr)	q(C)	δ(C,O)
(a) ae/AS	1.141	1,129.03	0.2	0.98	1.96
(a) ae/VS					1.96
(a) fc/VS	1.140	1,251.76	0.2	0.95	1.96
(b) ae/AS	1.137	1,118.46	0.2	0.96	1.94
(b) ae/VS			0.2		1.94
(b) ae/AS			0.1	1.08	1.89
(b) ae/VS			0.1		1.89
(b) fc/VS	1.136	1,148.62	0.1	1.07	1.89
(c)	1.114			–	1.51/1.52
(d)	1.126			1.15	1.80
(e)	1.103			1.35	1.57
(f)	1.128			1.16	1.80

See text for the details of the DFT calculations. The meaning of symbols are: *HF-SCF* Hartree-Fock self-consistent field calculation, *DFT* density functional theory, *B3LYP* exchange correlation functional [50], *PBE* Exchange correlation functional [35], *TZP* basis-set triple-ζ with polarization, *TZ2P* triple-ζ with double polarization, *ae* all-electrons, *fc* frozen cores, *AS* all KS MOs used in Eq. 2, *VS* only valence KS MOs used in Eq. 2, ΔE is the dissociation energy, q(C) is the charge (in e^- units) in the C basin. (a) DFT-PBE/TZP, this work; (b) DFT-PBE/TZ2P, this work; (c) HF-SCF/6−31G* /HF-SCF/6−31++G**, Ref. [16]; (d) DFT-B3LYP/6-311++G(2d,2p), Ref. [20]; (e) HF-SCF/6-311++G(2d,2p), Ref. [20]; (f) HF-SCF/QCISD/ae, Ref. [45]

Table 2 Delocalization index and basin population for the isolated CO molecule calculated with PW basis-sets with different density energy-cutoff in a cubic cell with PBC

Density energy-cutoff	Cell side (Å)	ΔE (kJ/mol)	Side of elementary volume (bohr)	q(C)	δ(C,O)
250	7	1,113.44	0.18	1.19	1.72
500	7	1,108.90	0.14	1.20	1.71
1,200	7	1,108.89	0.088	1.20	1.72
1,400	7	1,108.89	0.083	1.20	1.72
250	8	1,097.29	0.18	1.19	1.72
250	9	1,100.76	0.18	1.19	1.72
250	10	1,100.59	0.18	1.20	1.72

The C–O distance is 1.140 Å (the energy minimum for the energy-cutoff of 250 Ry with cell size of 7 Å). ΔE is the dissociation energy; q(C) is the charge (in e^- units) in the C basin

using different accuracy in the PW basis-set, keeping the same approximations for the electron density description (DFT) and for the exchange–correlation functional (PBE) used with localized basis-sets. With this set-up, the atomic cores are approximated via ultrasoft pseudopotentials, that may be compared with frozen-core approximation in the localized basis-set context. We remind that the core electron density is smoothly added to the valence electron density for the QTAIM analysis (see Sect. 2 for details).

As displayed in Table 2, the DI of CO does not change when the side of the elementary cube in the integrals is decreased in the range of 0.2–0.1 bohr, thus showing a negligible improvement with the 3-d grid resolution. The difference of PW result (1.72) and the accurate calculation of Refs. [20, 45] (1.80) is within 0.1 units, i.e., within the error attributed to the 3-d grid largest resolution available with localized basis-sets (see Table 1). Even though the dissociation energy is slightly affected by the cell size, the covalent bond character of the bond is identical by changing both cell size and 3-d grid density.

The residual difference between δ(C,O) obtained with the PW and localized basis-sets, 1.7 and 1.8, respectively, can be attributed to the difference in the approximations used, in the two methods, for core electrons. Since different approaches for core electrons when a PW basis-set is used (like norm-conserving pseudopotentials) provide results very similar to those obtained with ultrasoft pseudopotentials (data not shown here), this residual difference denotes a larger electrostatic character for PW representation of polar bonds, compared to localized basis-sets (see also below).

In order to test the convergence of PW and localized basis-sets for charged molecules, the case of cyanide was investigated in more detail. The problem of computing accurate electron density and energy for simple charged molecules when a PW basis-set is used within DFT method, has been already discussed and suitable corrections have been proposed [32, 33]. In the following, we present results obtained with different levels of accuracy in the calculation, summarized in Table 3.

Table 3 Delocalization index, δ in Eq. (2), for CN^- and NaCN (isolated and in the *fcc* lattice)

Set-up	Code	Pair	Distance (Å)	δ
(a)	Gaussian	C–N	1.172	2.45
TZ2P ae	ADF	C–N	1.184	2.43
TZ2P fc	ADF	C–N	1.183	2.43
PBE-US	QE	C–N	1.182	2.34
PBE-US-Corr1	QE	C–N	1.182	2.32
PBE-US-Corr2	QE	C–N	1.182	2.27
PBE-US (NaCN isolated)	QE	C–N	1.182	2.20
		Na–C/N	>4.1	0.37
PBE-US (NaCN crystal)	QE	C–N	1.18	2.13–2.46
1 cell		Na–C/N	>2.59	<0.18
PBE-US (NaCN crystal)	QE	C–N	1.18	2.12–2.29
2 cells	QE	Na-C/N	>2.59	<0.1

See Sect. 2 for the details of the DFT calculations. The meaning of symbols are: *TZ2P* Slater-type orbitals triple-ζ double-polarization basis-set, *ADF* Amsterdam density functional code [43], *ae* all-electrons, *fc* frozen cores (only valence electrons), *QE* Quantum-Espresso code [31], *PBE* Perdew–Burke–Ernzerhof exchange-correlation functional [35], *US* ultrasoft pseudopotential [6], *Corr1* correction of density and electrostatic potential based on Ref. [32], *Corr2* correction of density and electrostatic potential based on open boundary conditions [33]; (a) DFT-B3LYP/6-311++G(2d,2p) basis-set, Ref. [20]

Similarly to the CO case (see Table 2), the value of DI for cyanide in the energy minimum (Table 3) does not depend on the size of the PW basis-set (i.e., the 3-d grid resolution), being the value identical increasing the PW energy cut-off to 50 Ry for wave functions and to 400 Ry for the density (data not shown). Moreover, the DI is almost unaffected by the accurate correction to electron density and atomic forces, like that reported in Refs. [32] and [33] (see Table 3), being the variation in the range of

0.1 units. With the addition of one Na atom to the super-cell (the charge of which being zero), at a distance larger than 4 Å from the closer CN atom (the NaCN isolated case), the DI of the C–N pair is very close to that obtained with the negative cyanide super-cell (2.20 and 2.34, respectively). The geometry optimization of a single cell of the crystalline NaCN in the *fcc* lattice with the cell parameters of KCN [46] (the NaCN crystal case) provides a larger range for δ(C,N) when a single cell is used. We remind that in all cases examined in this work the systems are all periodical in the three directions of space. The unitary cell of NaCN contains four NaCN units and part of the variability in DI is due to the presence of four non-equivalent C–N pairs. In the single cell example, a small DI value is measured also for Na–C/N pairs (the maximal value is 0.18 for pairs of atoms at the minimal distance of 2.59 Å). As it is observed for NaCl (see Table 4 and related discussion), the convergence of DI for polarized extended electron densities requires more than one unit cell. Indeed, with an array of $2 \times 2 \times 2$ unitary cells, the delocalization of pairs involving Na becomes lower than 0.1. The charge in the Na basins is rather independent from the super-cell size, being 0.88 for a single unitary cell and 0.89 when 8 unitary cells are used in the calculation. The difference of q(Na) from unity (the value expected for an ideal ionic state) is due to the large number of small ($\delta < 0.1$) DIs involving each Na atom: the sum of the 8 DIs with $0.01 < \delta(\mathrm{Na,X}) < 0.1$ (in the range of 0.014–0.038) for each Na atom, is about 0.1.

Interestingly, all the types of cell neutralization have almost no effect on the delocalization between C and N. The major effect on δ(C,N) (0.2 units) arises from statistical errors that put independent estimates (nonequivalent C–N pairs at covalent contact) in the range of 2.1–2.3 units (bottom of Table 3). This range is consistent with an error of 0.1 units on each measure.

A final assessment of the PW calculation of DIs is the of DI upon molecule dissociation. To investigate this issue, the electron density and KS MOs of the CO molecule were computed as a function of the C–O distance (in the range of 1–4 Å), in different spin configurations (values of S_z) and with localized and PW basis-sets. The difference in dissociation energy between the TZ2P/fc basis-set and the PW calculation is within about 40 kJ/mol (1,149 and 1,113 kJ/mol, respectively, see Tables 1, 2). The behavior of δ(C,O) as a function of C–O distance (data not shown) shows that, with both basis-sets, a distance of 2.5 Å is necessary to have δ(C,O) smaller than 0.1, and, in both cases, this occurs in the $S_z = 2$ spin configuration. Indeed, the correct description of CO dissociation requires the use of $S_z = 2$ at the unrestricted level because both the C and O isolated atoms have triplet ground states. With other values of S_z, complex spin-couplings would occur which could be correctly resolved only at the full configuration interaction level. Since the spin polarization density is uniformly shared between the C and O atomic basis upon dissociation, the dissociation is homolytic. In both basis-sets, the molecular dipole points C along the whole dissociation. The positive charge in the C basin of the relaxed state was 1.2 for PW and 1.1 for TZ2P/fc basis-sets, respectively (see Tables 1, 2), and became zero beyond the critical 2.5 Å distance in both basis-sets. The PW description, as already

Table 4 Delocalization index, δ in Eq. (2), for simple molecules and for NaCl and LiF in the *fcc* lattice

Molecule	DFT PW	DFT localized: Gaussian (a, b, c) or Slater (d) type basis-set in the frozen-core approximation
H_2	1.00	1.00 (a)
N_2	3.00	3.05 (a)
F_2	1.28	1.28 (a)
CO	1.72	1.81 (a)/1.80 (c)/1.89 (d)
CN^-	2.34	2.45 (a)/2.43 (d)
NO^+	2.30	2.66 (a)/2.65 (d)
C_2H_6 (C–C)	1.04	1.01 (c)/1.02 (d)
C_2H_6 (C–H)	0.96	0.96 (d)
C_2H_4 (C–C)	1.93	1.90 (c)/1.88 (d)
C_2H_4 (C–H)	0.95	0.97 (d)
C_2H_2 (C–C)	2.85	2.85 (c)/2.80 (d)
C_2H_2 (C–H)	0.91	0.94 (d)
C_6H_6 (C–C ortho)	1.39	1.40 (b)
C_6H_6 (C–C para)	0.11	0.11 (b)
NaCl	0.074 ÷ 0.083	–
LiF	0.048 ÷ 0.051	0.221 (a)

See text for the details of the DFT calculations. (a) DFT-B3LYP/6-311++G(2d,2p) basis-set, Ref. [20] (LiF is the isolated molecule); (b) HF-SCF/3-21G*, Ref. [47]; (c) DFT-B3LYP/6-311++G(p,d,f) basis-set, HF-SCF at QCISD/ae level, Ref. [45]; (d) DFT-PBE/TZ2P all-electrons, this work

observed comparing q(C) in Tables 1 and 2, is slightly more polarized than that represented via localized basis-sets (the electron sharing is more toward a ionic state).

This type of in vacuo homolytic dissociation is rarely encountered during first-principle simulations in condensed phases, where atoms can exchange bonds between each other and, indeed, chemical bonds can break and form during molecular dynamics simulations performed at the DFT level, smoothly displacing electron pairs between different atomic pairs. The above convergence analysis shows that the set-up for low resolution PW calculations usual for first-principle computer simulations, that is a density energy cut-off of 250 Ry (a spatial resolution of KS MOs of 10 pm) and the use of ultrasoft pseudopotential for atomic cores, provides measures of electron sharing between atoms of accuracy comparable with routine methods of quantum chemistry. This set-up will be used in the following applications.

3.2 Applications to simple molecules

In Table 4, the delocalization indices for several simple molecules, with atomic coordinates of energy minima, are reported. For comparison with localized basis-sets, former results reported in the literature [20, 47] are displayed when available, and results obtained with ADF [43], elaborated as explained in the Sect. 2, are reported for the other cases. The table shows that the agreement between DIs computed with PW and localized basis-sets (expanded in gaussian functions or in Slater functions) is excellent in most of the cases, also when delocalization is significant (like in benzene). The largest discrepancy is observed for polar and charged molecules (LiF and NO^+). By comparing DIs for ethane, ethene, and ethine molecules, it can be noticed that the 2- and 3-bonding character of C–C pairs is well captured. The different estimate of electron sharing in heteroatomic bonds when the PW approach is adopted in place of the localized basis-set, is related to a larger polarization (a more "electrostatic" character) of these bonds in the PW description. Interestingly, the order $\delta(N_2) > \delta(NO^+) \sim \delta(CN^-) > \delta(CO)$ for this series of isoelectronic species is preserved irrespective of the method and basis-set used. The DI decreases from N_2 to CO along the isoelectronic series with the increased electronegativity difference (greater charge transfer and polarization) of the atoms involved in the bond. As for the sensitivity of DIs to the level of theory in the calculation of the electronic ground state, we notice that the Hartree–Fock calculation of DIs for CO, CN^- and NO^+, performed with the 6-311++G(2d,2p) basis-set, provided 1.6, 2.2, and 2.4, respectively [20], i.e., values slightly smaller than those provided by DFT with the same basis-set. Noticeably, this change is larger than that caused by the use of PW in representing the KS MOs.

The larger emphasis for the electrostatic character of polar interactions when PW basis-set is used, is shown also by other polarized systems in Table 4. For both NaCl and LiF, the upper limit for δ(A,B) is 0.1 when 8 unitary cells are assembled in the $2 \times 2 \times 2$ super-cells, while the maximal value of 0.35 is obtained with a single unitary cell (data not shown). Moreover, this upper limit is not for pairs involving atoms with opposite formal charges (the numbers displayed in Table 4), but it holds for pairs of formal anions at the closest distance. Large assemblies of cells or, alternatively, a set of $K > 0$ values, must be used for extended systems in periodic lattices. Even if a significant electron sharing has been observed also for ionic molecules, like the isolated LiF molecule [20], accurate assessment of DIs for extended systems deserve a complete relaxation of the cell size and shape, possibly using all the information of the lattice periodicity. In the usual PW expansion, the use of $K > 0$ values impose constraints in the symmetry of the KS MOs that must be taken into account before using Eq. (2). The complete use of lattice periodicity is the subject of a further elaboration of Eq. (2). In this work, we limit the use of the equation to lattice periodicity with length-scales not larger than the super-cell dimensions (see Sect. 2).

If cell relaxation is not fully accomplished, the sensitivity of the measure of DIs based on PW expansions of KS MOs is assumed to be 0.1: all the DIs smaller than 0.1 cannot be safely interpreted as sharing of electrons without a complete relaxation of the cell containing the atoms and a full assessment of the convergence of DIs as functions of the finite element size in electron density 3-d representation.

The measure of DI for the H_2^+ molecule in the ground state is 0.5 for all basis-sets, including PW, and it is fully consistent with the exact MO and valence bond theories, both based on the description of energy eigenstates as combinations of atomic orbitals. We remark here that by using the equation for DIs (Eq. 2), DIs are always positive and are not able to distinguish between bonding and antibonding states. The indices are, therefore, merely descriptive and not predictive. Nevertheless, the behavior of DIs upon chemical substitution provides a conceptual frame for measuring the modification of electronic structure. Moreover, the combination of these indices for electron sharing with atomic forces, both measured within the same theoretical framework, provides a unified description of molecular dynamics and of electronic ground state, without the need of an atom-centered basis-set.

3.3 Applications to metal complexes

In Table 5 DIs for Fe complexes with CO (charge zero) $Fe(CO)_5$ (trigonal bi-pyramidal) and $Fe(CN)_6^{4-}$ (octahedral) are displayed. The agreement for the CO complex

Table 5 Delocalization index, δ in Eq. (2), for simple molecules with metal-C bonds ($Fe(CO)_5$ and $Fe(CN)_6^{4-}$)

Molecule	Bond	DFT PW	DFT localized: Gaussian (a) or Slater (b) type basis-set
$Fe(CO)_5$	$Fe–C_{eq}$	1.05–1.06	1.05 (a)/1.09 (b)
	$Fe–C_{ax}$	0.99	0.98 (a)/1.04 (b)
	$C_{eq}–O_{eq}$	1.55–1.75	1.61 (a)/1.64–1.68 (b)
	$C_{ax}–O_{ax}$	1.55–1.76	1.61 (a)/1.68 (b)
	$Fe–O_{eq}$	0.20	0.18 (a)/0.20 (b)
	$Fe–O_{ax}$	0.19	0.17 (a)/0.19 (b)
	$C_{eq}–C_{ax}$	0.15	0.13 (b)
$Fe(CN)_6^{4-}$	Fe–C	0.72–0.73	0.80 (b)
	C–N	2.00–2.38	2.25 (b)
	Fe–N	<0.1	0.15 (b)

See text for the details of the DFT calculations. (a) DFT-B3LYP/6-311++G(p,d,f) basis-set, Ref. [45]; (b) DFT/PBE/TZ2P/ae, this work

between the two basis-sets is excellent for all the atomic pairs. Noticeably, even the low DIs between the axial and equatorial C ligand atoms is captured in both representations of the electronic structure, as well as the small three-center four-electrons (3c-4e) sharing represented by the Fe–O pairs. No DIs are detectable for O–O pairs.

The discrepancy between the representations for the cyanide Fe complex are due to the need of an unrestricted spin calculation for the PW representation only. Because of the constraint of O_h symmetry that can be explicitly imposed with the atom-centered basis-set, the restricted calculation was possible only in this latter case. Molecular symmetry cannot be constrained in PW calculations.

However, the average value for Fe–C and C–N pairs are within 0.1 units in the two representations and the major difference is concentrated in the Fe–N pairs that, again, in the PW representation with core pseudopotential, is less covalent in character.

3.4 Applications to M–M bonds

In the following, calculations of DIs for systems containing several metal atom centers are performed in terms of PW representations of KS MOs and compared with the same calculation performed with localized atom-centered basis-sets.

The measure of DIs involving metal atoms and metal–metal bonds has been performed in a few cases [45, 48]. In this work, the DIs are computed for the $Pt_3(CO)_6^{2-}$ anion. This anion is stable in solution, while it forms different kinds of assemblies in solution and in the solid state (see Ref. [34] and references therein). The monomeric anion is planar (D_{3h} space group in the crystalline solid state).

In Fig. 1 the energy minimized configuration of the monomeric anion, in a super-cell mimicking the isolated state, is displayed (the program VMD [49] is used in all the molecular drawings). The Pt–Pt distance is 2.68 Å. The DIs are summarized in Fig. 2 for all the atomic pairs with DI

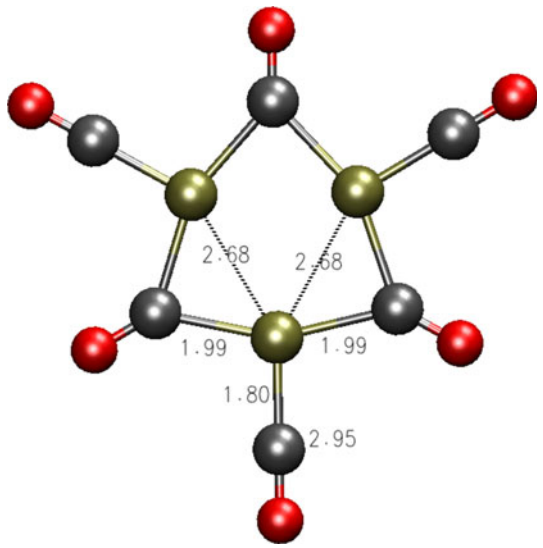

Fig. 1 Energy minimized structure of the $Pt_3(CO)_6^{2-}$ anion. Color scheme is the following: Pt atoms are in *gold*, C in *gray*, O in *red*. Bonds are drawn for guiding the eye. The VMD program [49] was used for this drawing

larger than 0.1 units. The range of computed values is indicated, with different values corresponding to pairs equivalent by symmetry. The subscript t and b indicates, respectively, terminal and bridging CO groups.

The data reported on the scheme of Fig. 2 show that the bond structure revealed by DIs is consistent with a widely delocalized electron structure. The electron sharing between the atoms O_t and Pt (0.3) is an indication of 3c-4e bonding interaction, implying an electron sharing more significant than the 3c-4e sharing in $Fe(CO)_5$ (see Table 5). This value is identical to the value of 0.3 measured for the pair O–O′ in CO_2 [20]. The 3c-4e Pt–O_t bonds arise from Eq. (2) when the major contribution to the sum is from MOs composed by atomic orbitals centered on two different atoms separated by an other atom, as is the case for the π_g molecular orbital in CO_2. If the three Pt atoms

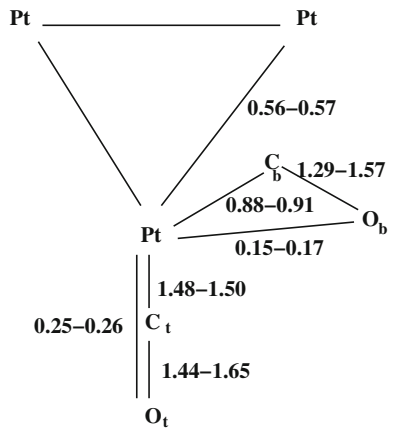

Fig. 2 DIs for $Pt_3(CO)_6^{2-}$ anion. DIs ≤ 0.1 are omitted

identify the *xy* plane, the p_z orbitals of O, and the $d_{x/yz}$ orbitals of Pt contribute to the occupied weakly antibonding states of relatively high energy. Noticeably, this effect is also represented in the PW basis-set.

The sum of DIs involving one Pt atom is at least 4.9. This means that at least $4.9/2 = 2.45$ over 10 valence electrons are scattered by each Pt atom within the Pt_3 plane and mainly shared with CO ligands via covalent bonds (or "Lewis-type" pairs).

In order to see how the DIs are affected by fluctuations due to thermal motions, the calculation of DIs was repeated on the electron density following the time evolution of a typical molecular dynamics simulation at the temperature $T = 300$K (data not shown). Even if all the distances fluctuate significantly (for instance Pt–Pt distances oscillates within 2.7 and 2.9 Å) the DIs are subject to small variations, within ± 0.2 units. The root-mean square error between DIs for a snapshot at $T = 300$K and the initial configuration (that displayed in Figs. 1, 2) is 0.1. This observation confirms that, as far as the molecule does not change its topology (i.e., when no chemical reactions occur), the DIs can be used as covalent (or "Lewis-type") bond indices, being the changes in DIs during atomic motions of the same size of the sensitivity of the method (0.1, see Sect. 3.1 about the convergence of results).

4 Conclusions

The delocalization indices have been computed on the basis of DFT calculations where the Kohn–Sham molecular orbitals are represented in terms of plane waves and where the size of the finite element representing 3-d real-space electron density and Kohn–Sham molecular orbitals is in the range of 10 pm. Delocalization indices computed with this method are in agreement with those computed on the basis of localized basis-sets of routine usage in quantum chemistry. Delocalization indices measure the number of shared electrons between the involved atoms, thus they provide a reliable estimate of the covalent character of chemical bonds in atomic assemblies ranging from isolated molecules to extended atomic clusters and infinite aggregates, these latter represented within periodic boundary conditions and represented at the same 3-d spatial resolution used in this work for simple molecules.

Acknowledgments This work has been performed under the HPC-EUROPA2 project (project number: 127) with the support of the European Commission—Capacities Area—Research Infrastructures. MS acknowledges financial support from the Spanish MICINN project nr. CTQ2008-03077/BQU and the Catalan DIUE through project nr. 2009SGR637. Support for the research of MS was also received through the prize "ICREA Academia" 2009 for excellence in research funded by the DIUE of the Generalitat da Catalunya. GLP thanks P. Giannozzi (University of Udine, Italy) for the many suggestions.

Note added in proof

Soon after the paper was accepted, it appeared a work by Baranov and Kohout (Barnanov AI, Kohout M (2011) J Comput Chem DOI: 10.1002/jcc.21784) that discusses the calculation of electron localization and delocalization indices in solid state periodic systems using plane waves and the QTAIM partition.

References

1. Parr RG, Yang W (1989) Density functional theory of atoms and molecules. Oxford University Press, New York
2. Grotendorst J (ed) (2000) NIC series: modern methods and algorithms of quantum chemistry, vol 3. John von Neumann Institute for Computing, FZ Jülich (DE)
3. Cramer CJ, Truhlar DG (2009) Phys Chem Chem Phys 11:10757–10816
4. Hohenberg P, Kohn W (1964) Phys Rev B 136:864–871
5. Kohn W, Sham LJ (1965) Phys Rev A 140:1133–1138
6. Vanderbilt D (1990) Phys Rev B 41:7892–7895
7. Giannozzi P, De Angelis F, Car R (2004) J Chem Phys 120:5903–5915
8. Car R, Parrinello M (1985) Phys Rev Lett 55:2471–2474
9. Hoffmann R (1988) Solids and surfaces: a chemist's view of bonding in extended structures. Wiley-VCH, New York
10. Matta CF, Boyd RJ (eds) (2007) Quantum theory of atoms in molecules: from solid state to DNA and drug design. Wiley-VCH Verlag GmbH & Co. KGaA, Weinheim
11. Sjöstedt E, Nordström L, Singh DJ (2000) Solid State Commun 114:15–20
12. Otero-de-la-Roza A, Blanco M, Martín Pendás A, Luaña V (2009) Comput Phys Commun 180:157–166
13. Evarestov RA, Tupitsyn II, Bandura AV, Alexandrov VE (2006) Int J Quantum Chem 106:2191–2200
14. Bader RFW, Stephens ME (1975) J Am Chem Soc 97:7391–7399
15. Fulton R (1993) J Phys Chem 97:7516–7529
16. Ángyán JG, Loos M, Mayer I (1994) J Phys Chem 98:5244–5248
17. Fradera X, Austen MA, Bader RFW (1999) J Phys Chem A 103:304–314
18. Silvi B (2004) Phys Chem Chem Phys 6:256–260
19. Poater J, Duran M, Solà M, Silvi B (2005) Chem Rev 105:3911–3947

20. Fradera X, Poater J, Simon S, Duran M, Solà M (2002) Theor Chem Acc 108:214–224
21. Matito E, Solà M, Salvador P, Duran M (2007) Faraday Discuss 135:325–345
22. Borisova NP, Semenov SG (1973) Vestn. Leningr Univ (16):119–126
23. Kar T, Ángyán JG, Sannigrahi AB (2000) J Phys Chem A 104:9953–9963
24. Mayer I (2007) J Comput Chem 28:204–224
25. Parr RG, Ayers PW, Nalewajski RF (2005) J Phys Chem A 109:3957–3959
26. Bader RFW (1990) Atoms in molecules—a quantum theory. Oxford University Press, Oxford
27. Matito E, Poater J, Solà M, Duran M, Salvador P (2005) J Phys Chem A 109:9904–9910
28. Bultinck P, Cooper DL, Ponec R (2010) J Phys Chem A 114:8754–8763
29. Bertini L, Cargnoni F, Gatti C (2007) Theor Chem Acc 117:847–884
30. Dovesi R, Saunders VR, Roetti R, Orlando R, Zicovich-Wilson CM, Pascale F, Civalleri B, Doll K, M HN, J BI, D'Arco P, Llunell M (2009) CRYSTAL09. University of Torino, Italy. http://www.crystal.unito.it
31. Giannozzi P, Baroni S, Bonini N, Calandra M, Car R, Cavazzoni C, Ceresoli D, Chiarotti GL, Cococcioni M, Dabo I, Dal Corso A, de Gironcoli S, Fabris S, Fratesi G, Gebauer R, Gerstmann U, Gougoussis C, Kokalj A, Lazzeri M, Martin-Samos L, Marzari N, Mauri F, Mazzarello R, Paolini S, Pasquarello A, Paulatto L, Sbraccia C, Scandolo S, Sclauzero G, Seitsonen AP, Smogunov A, Umari P, Wentzcovitch RM (2009) J Phys Condens Matter 21:395502. http://www.quantum-espresso.org
32. Martyna GJ, Tuckerman ME (1999) J Chem Phys 110:2810–2821
33. Dabo I, Kozinsky B, Singh-Miller NE, Marzari N (2008) Phys Rev B 77:115139
34. Femoni C, Kaswalder F, Iapalucci MC, Longoni G, Mehlstäubl M, Zacchini S, Ceriotti A (2006) Angew Chem Int Ed 45:2060–2062
35. Perdew JP, Burke K, Ernzerhof M (1996) Phys Rev Lett 77:3865–3868
36. Wolf D, Keblinski P, Phillpot SR, Eggebrecht J (1999) J Chem Phys 110:8254–8282
37. Makov G, Payne MC (1995) Phys Rev B 51:4014–4022
38. Sanville E, Kenny SD, Smith R, Henkelman G (2007) J Comp Chem 28:899–908 http://theory.cm.utexas.edu/bader/
39. Tang W, Sanville E, Henkelman G (2009) J Phys Condens Matter 21:084204
40. Zener C (1930) Phys Rev 36:51–56
41. Slater J (1930) Phys Rev 36:57–64
42. Eyring H, Walter J, Kimball G (1944) Quantum chemistry. Wiley, New York
43. te Velde G, Bickelhaupt F, van Gisbergen S, Fonseca Guerra C, Baerends E, Snijders J, Ziegler T (2001) J Comp Chem 22:931–967
44. Michalak A, DeKock RL, Ziegler T (2008) J Phys Chem A 112:7256–7263
45. Macchi P, Sironi A (2003) Coord Chem Rev 238–239:383–412
46. Stokes HT, Decker DL, Nelson HM, Jorgensen JD (1993) Phys Rev B 47:11082–11092
47. Poater J, Fradera X, Duran M, Solà M (2003) Chem Eur J 9:400–406
48. Matito E, Solà M (2009) Coord Chem Rev 253:647–665
49. Humphrey W, Dalke A, Schulten K (1996) J Molec Graphics 14:33–38. http://www.ks.uiuc.edu/Research/vmd
50. Becke AD (1993) J Chem Phys 98:5648–5652